Thermophysical Properties of Liquid Undercooled $Co_{80}Pd_{20}$ [1]

G. Lohöfer[2,3], S. Schneider[2], and I. Egry[2]

ABSTRACT

Surface tension, viscosity, and electrical resistivity of liquid $Co_{80}Pd_{20}$ were measured containerlessly for temperatures above and especially below the melting point. The first two quantities were measured with help of the oscillating drop technique, the last one by an inductive method. The experiments have been performed under low gravity in the electromagnetic levitation facility TEMPUS during the MSL-1 Spacelab mission. This environment allowed for the first time to measure the viscosity and electrical resistivity in the deeply undercooled state, where the $Co_{80}Pd_{20}$ melt shows a magnetic ordering behavior. In this paper the measurement methods and results are presented.

KEY WORDS: containerless, electromagnetic levitation, electrical resistivity, liquid, micro-gravity, surface tension, undercooled, viscosity.

---

1. INTRODUCTION

The Curie temperatures T_C of all known ferromagnetic metallic materials are lower than their liquidus temperatures T_l. This is why ferromagnetism is not observed in stable metallic melts. However by application of contactless positioning and measurement techniques, metallic melts can be undercooled significantly below T_l. Experiments on $Co_{80}Pd_{20}$ melts undercooled containerlessly close to T_C showed an attractive interaction between the melt and an external magnet [1]. Measurement of the temperature dependence of the magnetization by a Faraday balance on levitated undercooled drops [2] revealed a Curie-Weiss behavior with a Curie temperature of the liquid T_C^l being 20 K below that of the solid T_C^s. The magnetization steeply rises if the temperature is approaching T_C^l from above. From the theoretical point of view magnetic ordering in fluid matter is discussed recently with respect to the order-disorder transition [3] and the spatial structure of the liquid [4]. The sudden structural change in the undercooled $Co_{80}Pd_{20}$ melt with decreasing temperature should also result in a sudden change of its thermophysical properties. This was the motivation for us to measure the temperature dependence of surface tension, viscosity, and electrical conductivity of the liquid $Co_{80}Pd_{20}$ alloy in the metastable deeply undercooled state.

For undercooled metallic melts, where any mechanical contact with the material causes its immediate nucleation, containerless handling methods of the liquid as well as contactless measurement methods are mandatory [5]. But also for liquids above their melting points, especially for high temperatures or reactive materials, only noninvasive techniques can be applied for long duration measurements. The electromagnetic levitation is an established technique for containerless positioning and heating of metallic

melts by means of high frequency alternating magnetic fields $\mathbf{B}(x,t) = \mathbf{B}_0(x)\sin(\boldsymbol{w}t)$ [6], [7]. The levitation fields induce eddy currents in the sample. On the one hand these currents heat the sample due to Ohmic losses with the power

$$P \propto \mathbf{B}_0^2 . \tag{1}$$

On the other hand, their interactions with the original field produce Lorentz forces

$$\mathbf{F} \propto -\mathbf{B}_0 \cdot \nabla \mathbf{B}_0 \tag{2}$$

in direction of decreasing magnetic field strength, which support the sample against gravity and residual forces without any mechanical contact.

2. EXPERIMENT FACILITY

The experiments on $Co_{80}Pd_{20}$ have been performed under microgravity during two Spacelab missions (STS 83 and STS 94) in 1997 in TEMPUS, a facility for containerless, electromagnetic positioning and heating of metallic melts in low gravity. For the stable electromagnetic positioning of the sample TEMPUS uses a magnetic quadrupole field, produced by two parallel and coaxial coils carrying RF currents of the same strength but opposite direction. According to Eq. (2), the weightless metallic sphere is fixed in the center of the two coils where the magnetic field strength is just weakest, see Fig. 1. Since, moreover, the residual accelerations under microgravity, which have to be compensated by the positioning field, are relatively low ($< 10^{-3}$ g), the remaining magnetic field strength around a droplet can be decreased under microgravity conditions to values that are considerably weaker than those necessary to position the same sample against earth gravity. This has several experimental advantages:

- Under microgravity, bulk samples (in TEMPUS up to $\varnothing$ 8 mm) can easily be levi-

tated.

- According to Eq. (1), a low magnetic field strength results in a low heating power induced in the sample. This again renders possible to reach, even for low melting materials, deep undercoolings of metallic melts in an UHV environment. This is different to the situation on earth, where the high field strengths, necessary to position the droplet against gravity, usually require an additional convective gas cooling of the sample in order to reach temperatures below the melting point.

- Contrary to the situation under microgravity, where the very low and more continuously distributed magnetic force fields do practically not destroy the spherical shape of the droplet, on earth the sample deforms under its own weight. This prevents, however, simple and precise calculations of the specific material properties from the measurable quantities (see below).

- Another disadvantage originating from the high magnetic force field in electromagnetic levitation facilities on earth consists in the strong stirring of the liquid sample. That part of the magnetic force field that penetrates into the metal droplet generates turbulent fluid flows, which strongly disturb the viscosity measurement by the oscillating drop technique. Only the µg environment enables laminar flow fields in electromagnetically positioned liquid metal samples and thus allows the use of the oscillating drop technique for a containerless measurement of viscosities.
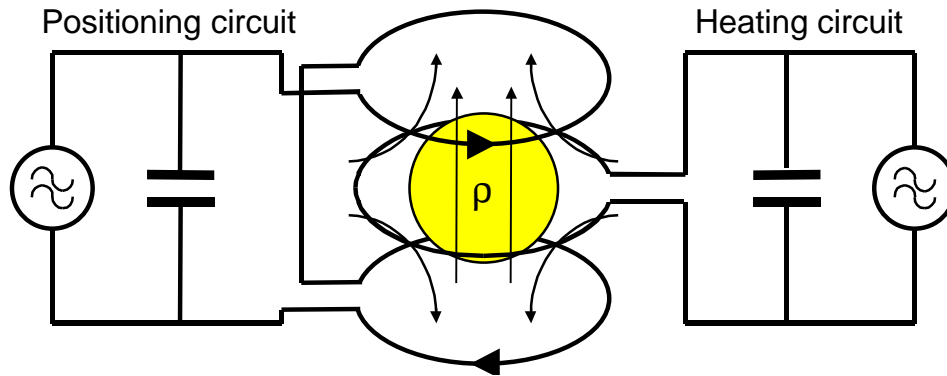
Fig. 1. Schematic sketch of the electrical oscillatory circuit arrangement including the positioning coil (above and below the sample) for the generation of an alternating (150 kHz) magnetic quadrupole field (curved arrows), and the heating coil (around the sample) for the generation of an alternating (350 kHz) magnetic dipole field (straight arrows). Each of the circuits has its own RF power supply.

On the other hand, the positioning of the sample in a region, where the magnetic field strength is just weakest, see Fig. 1, prevents an efficient heating and melting by the quadrupole field. Therefore, an additional "heating coil", connected with its own solid state generator for the RF current supply, has been provided in the TEMPUS facility. This coil produces a nearly homogeneous RF magnetic dipole field of high strength around the sample. The advantage of this coil arrangement is the possibility to control under microgravity the heating power and positioning forces of the sample almost independently of each other. The high efficiency and the homogeneity of the heating field enables also its use as measuring field for a containerless, inductive determination of the electrical sample resistivity.

3. MEASURING PRINCIPLES

3.1 Surface Tension and Viscosity

The oscillating drop method has been widely used to measure the surface tension of levitated liquid metals. This method makes use of the fact that the frequency of the surface oscillations of a liquid drop is related to the surface tension by Rayleigh's formula [8]. If the radius R of a spherical droplet undergoes free oscillations of the form:

$$R = R_0 (1 + \boldsymbol{d} \cos(\boldsymbol{w}t) e^{-\Gamma t}) , \tag{3}$$

where $\boldsymbol{d}$ ($\boldsymbol{d} << 1$) is the normalized amplitude of the oscillation, $\boldsymbol{w}$ is the resonance frequency and $\boldsymbol{G}$ is the damping, then the $\boldsymbol{w}$ is given by:

$$\boldsymbol{w}^2 = \frac{32\boldsymbol{pg}}{3m} , \tag{4}$$

where $\boldsymbol{g}$ is the surface tension and m is the mass of the drop.

Unfortunately, Rayleigh's formula cannot be applied directly to oscillations of levitated drops. The influence of the external electromagnetic and gravitational fields must be taken into account. These fields lead to a splitting of the single frequency, predicted by Rayleigh's equation (4), into up to five frequencies, and a shift of the frequencies. Although an approximate correction has been worked out [9], it is advantageous to perform such experiments under microgravity, where both fields are negligibly small, and Rayleigh's formula is applicable directly. Figure 5 below shows, however, the good coincidence between the surface tension data of $Co_{80}Pd_{20}$ measured on ground with help of the correction formula of Ref. [9] and in space with help of Eq. (4).

In addition, the oscillating drop technique also yields the viscosity of the droplet. This idea is based on Kelvin's work on the oscillations of viscous drops [10]. He derived the following expression for the damping constant $\boldsymbol{G}$:

$$\Gamma = \frac{20\boldsymbol{p}}{3} \frac{\boldsymbol{h}\,R_0}{m}\,.$$ (5)

where $\boldsymbol{h}$ is the viscosity. Like Rayleigh's formula, this equation is only correct for spherical drops in the absence of external fields. Although attempts have been made to include the effect of the external fields on the damping constant [11], experiments under microgravity may in fact be the only possibility to apply this method. The main reason for this consists in the strong additional damping of the oscillating droplet by the highly turbulent fluid flow in the melt of electromagnetically levitated metal samples on ground. This damping mechanism dominates that one originating from the viscosity given in Eq. (5). It can be excluded, if the experiments are performed under microgravity, where the low magnetic field forces generate at most laminar fluid flows in the liquid metal samples.

3.2 Electrical Resistivity

The presence of an alternating magnetic heating field suggests to use this field simultaneously for a non-contact, inductive measurement of the electrical resistivity of the levitated metal sample. Placed in the TEMPUS heating coil the sample represents an additional, inductively coupled electric circuit (transformer), see Ref. [12] and Fig. 2, of resistance R_S and inductance L_S that changes the complex impedance of the coil into

$$Z_{coil}(\boldsymbol{r},\boldsymbol{w}) = R + i\boldsymbol{w}L + R_S(\boldsymbol{r},\boldsymbol{w}) + i\boldsymbol{w}L_S(\boldsymbol{r},\boldsymbol{w})\,.$$ (6)
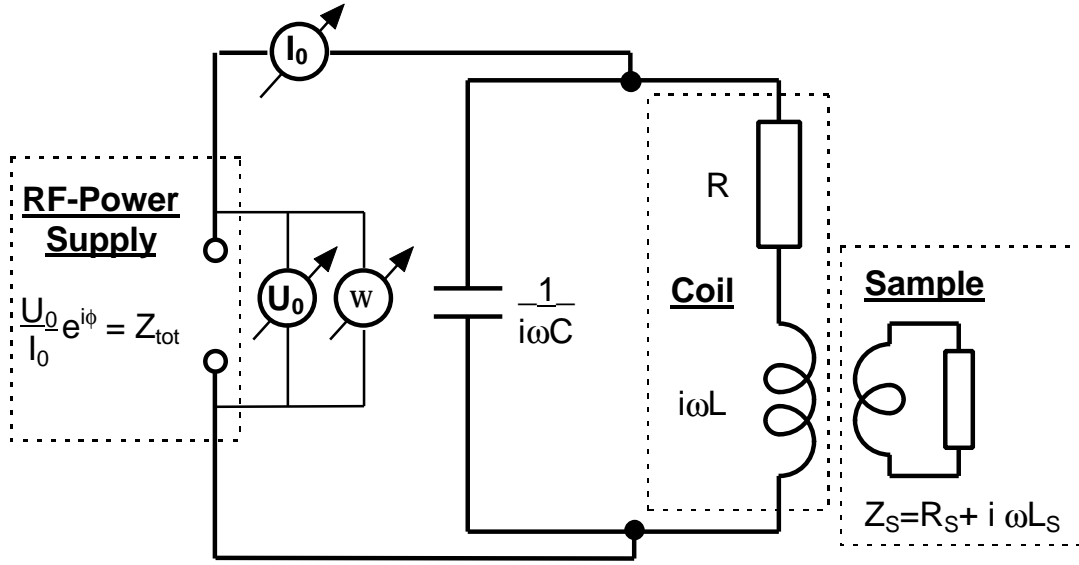
Fig. 2. Electrical wiring diagram of the TEMPUS oscillatory heating circuit, cf. Fig. 1, with inductively coupled sample circuit of impedance Z_S. The RF power supply feeds a current $I(t) = I_0 \sin(wt + f)$ at a voltage $U(t) = U_0 \sin(wt)$ into the heating circuit. I_0 and U_0 are recorded by the facility and used for the determination of the electrical sample resistivity.

More specifically, it increases the resistance R and decreases the inductance L of the empty coil. Both quantities are related to the sample resistivity r. Making use of the fact that the TEMPUS oscillatory heating circuit including the sample is only slightly damped, the relation between the real part of Z_{coil} and the measurable voltage amplitude U_0 across and current amplitude I_0 through the circuit as well as the phase difference f between U_0 and I_0 reads

$$\frac{C}{L}\left(R + R_S(r, w)\right) = \frac{I_0}{U_0} \cos(f) .$$

(7)

For the high magnetic field frequencies w of TEMPUS, for which the skin depth

$$d(r,w) := \sqrt{2\,r/(m_0 w)} \tag{8}$$

is small compared to the radius a of the spherical sample, the equation for the sample

resistance R_S assumes a relatively simple expression [12] and the relation between the

measurable quantities U_0, I_0, and f on the one hand and the electrical sample resistivity

r contained in $d(r,w)$, Eq. (8), on the other hand finally reads

$$d(r,w) = \frac{a}{2}\left(1 - \sqrt{1 - \frac{B}{a^3}\left(\frac{I_0}{U_0}\cos f - A\right)}\right). \tag{9}$$

Here A and B are constants which characterize the empty coil and which can be deter-

mined by calibration. A detailed description of the evaluation procedure is given in [13].

The simple expression of (9) supposes a spherical sample shape, which is essen-

tially realized under microgravity only. Furthermore, (9) also requires a homogeneous

dipole field around the sample, which is generated by the TEMPUS heating coil, but

which is generally not available in earthbound levitation facilities. We make attempts to

measure electrical resistivities also in earthbound levitation facilities [14]. This is, how-

ever, a complicated task mainly due to the not well defined, pearlike sample shape.

4. EXPERIMENT PERFORMANCE AND RESULTS

A typical experiment run in TEMPUS is shown in Fig. 3. The electromagneti-

cally positioned $Co_{80}Pd_{20}$ sample of 8 mm diameter is inductively heated, melted, and

overheated. It cools down after the heating power is turned down, undercools, solidifies,

where the latent heat release suddenly increases the temperature, and finally cools down

in the solid state. As the liquid droplet cools, short current pulses are sent through the

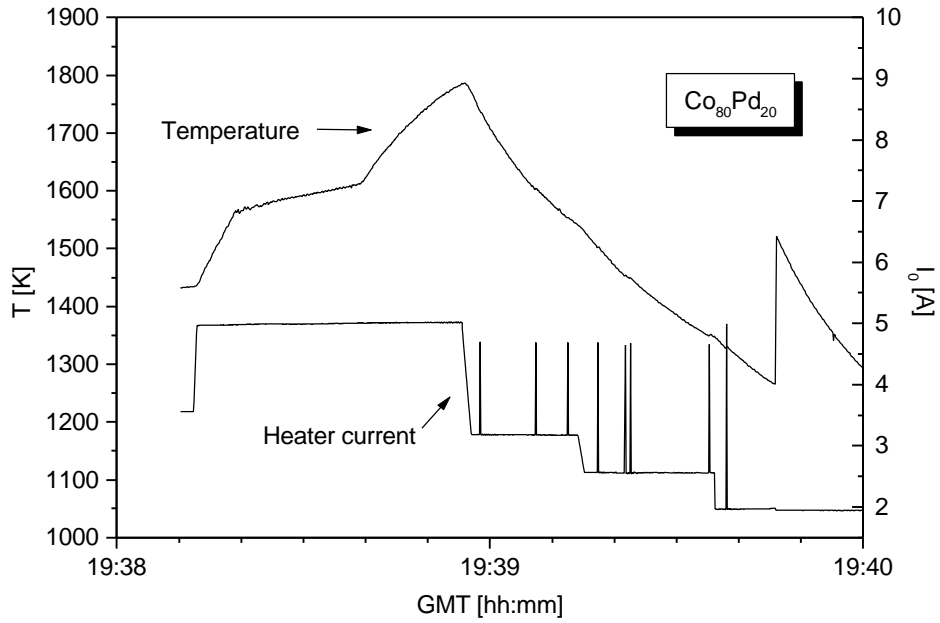heating coil, leading to a lateral compression of the sample and subsequent oscillations.

Fig. 3. Typical thermal cycle of the TEMPUS $Co_{80}Pd_{20}$ experiment. Plotted are the sample temperature and the current into the heating circuit. The spikes correspond to pulses used to excite surface oscillations in the melt, the damping of which is related to the viscosity.

Although observing the oscillations during cooling introduces a temperature error of about 5 - 10 K, it has the advantage that the electromagnetic fields are reduced to a minimum, eliminating any fluid flow effects. During one cooling cycle, such an excitation pulse was applied every 50 K, until the sample solidified. The video images were analyzed frame by frame and the radius of the sample was determined as a function of time. An example is shown in Fig. 4. The damping constant was obtained from the time signal directly, whereas the frequency was obtained from the Fourier transform of the signal.
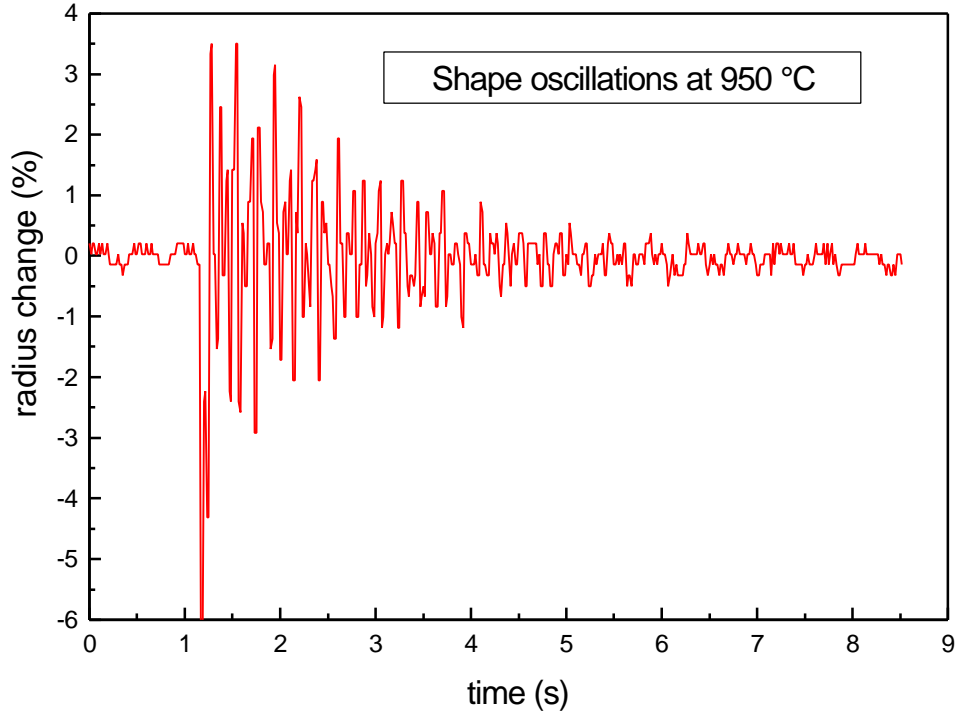
Fig. 4. Excitation and decay of a surface oscillation, as detected in the video signal.

During the whole thermal cycle the voltage amplitude U_0 across and the current amplitude I_0 through the circuit were automatically measured with a rate of 10 Hz. The phase difference f, also necessary to determine the electrical sample conductivity r, was fixed by the RF power supply. After the determination of the coil constants A and B by a previous calibration run, r was calculated from the measurement values via (8) and (9). Due to the high data rate we obtained a value of r every 1 K.

4.1 Surface Tension and Viscosity

Using Eqs. (4) and (5) to convert frequencies and damping constants into surface tension and viscosity, we have analyzed all oscillations and obtained surface tension and

viscosity as functions of temperature. The results are shown in Figs. 5 and 6, respectively.
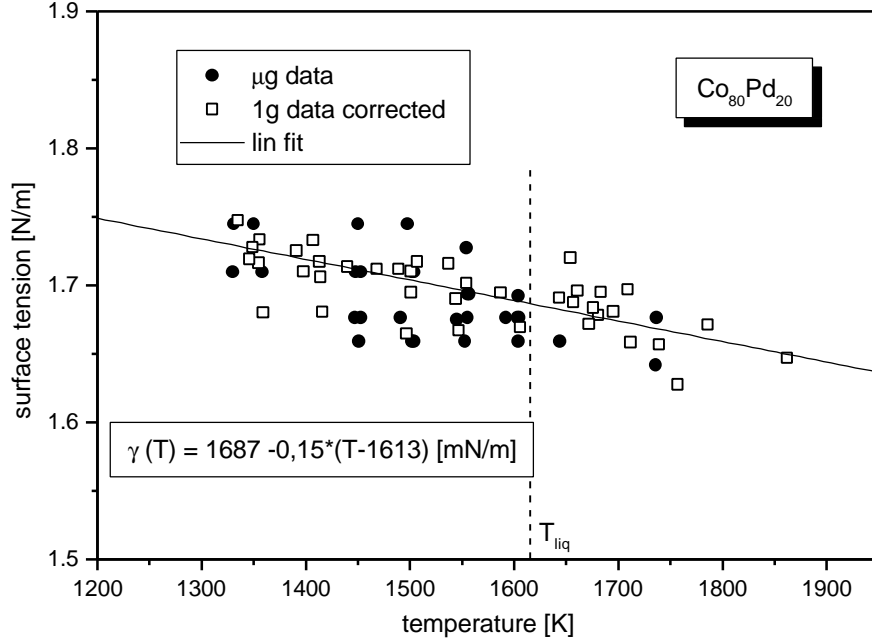

Fig. 5. Surface tension of $Co_{80}Pd_{20}$ as function of temperature. The vertical line represents the liquidus temperature. Besides the µg data measured in TEMPUS the plot also contains data that have been measured previously in our earthbound levitation facility by the same method. The 1g data have been corrected for the additional strong gravitational and electromagnetic forces on the sample.

The surface tension data have been fitted to a linear relation and we obtain:

$$\boldsymbol{g}_{Co_{80}Pd_{20}}(T) = 1.69 - 15 \cdot 10^{-5} \cdot (T - 1613) \quad [N/m], \tag{10}$$

where temperature T is in K. The viscosity was fitted to an Arrhenius type expression, yielding:

$$\mathbf{h}_{Co_{80}Pd_{20}}(T) = 0.15 \cdot \exp(6790/T) \quad [mPa \ s]. \tag{11}$$

The measured viscosities range from 5 to 30 mPa s, covering nearly an order of magnitude. An undercooling of approximately 300 K leads to an increase in viscosity by a factor of 3.
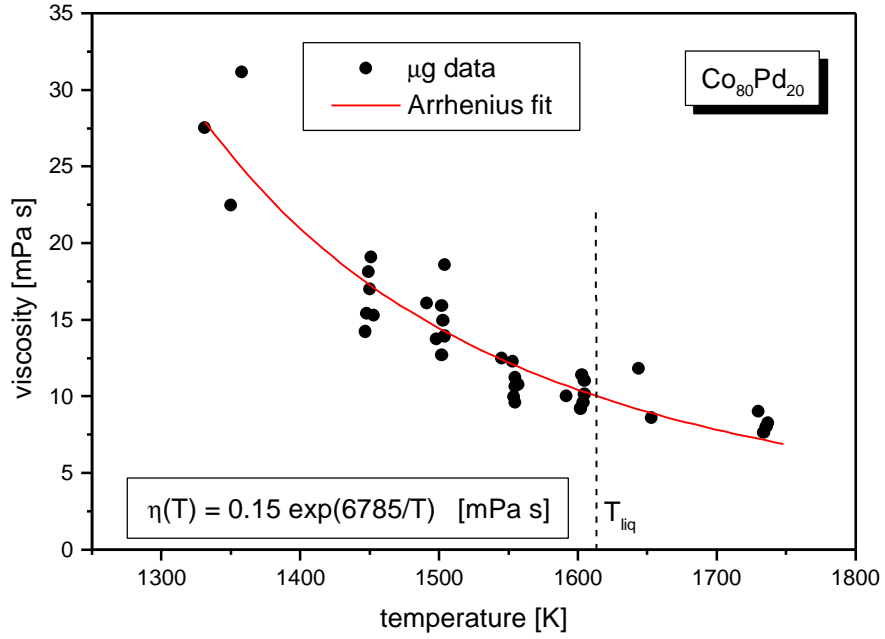

Fig. 6. Viscosity of $Co_{80}Pd_{20}$ as function of temperature. The vertical line represents the liquidus temperature. The data points are fitted to an Arrhenius law.

The drastic deviation of the resistivity data, presented in Fig. 7 below, from the linear temperature behavior shows very clearly the onset of the magnetic ordering in the undercooled $Co_{80}Pd_{20}$ melt at 1325 K. Unfortunately, this temperature represents also the lower limit of our measured surface tension and viscosity data, so that the expected

deviations from their typical temperature behaviors due to structural changes in the liquid could not be verified.

4.2 Electrical Resistivity

The evaluation of the voltage and current data from the TEMPUS $Co_{80}Pd_{20}$ viscosity experiment measured during the cooling phase of two thermal cycles including that one of Fig. 3, results in the resistivity diagram of Fig. 7.
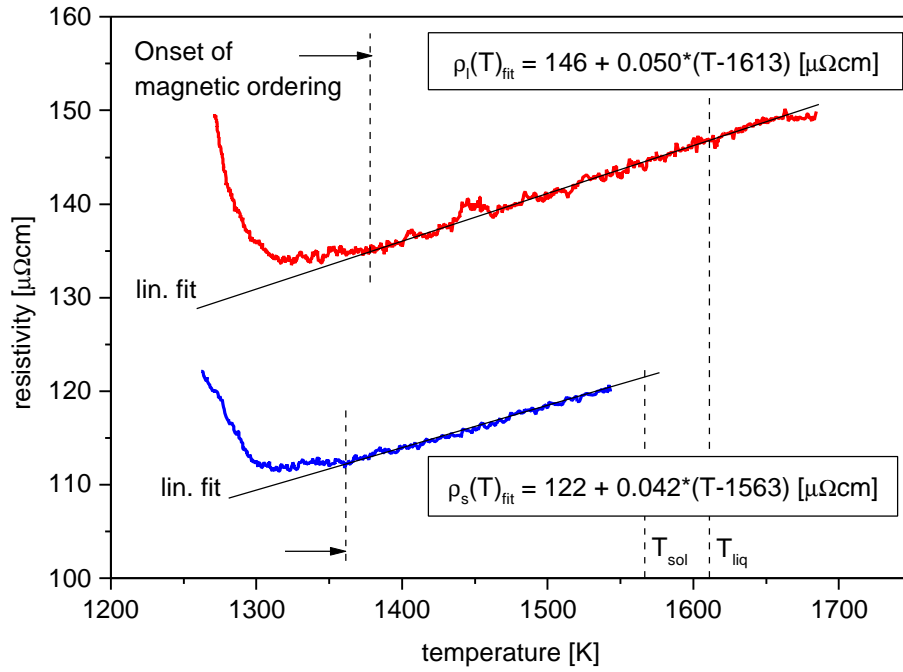

Fig. 7. Electrical resistivity r of $Co_{80}Pd_{20}$ in the solid (lower curve) and liquid (upper curve) state, together with the corresponding linear fits as function of the temperature T. T_{sol} and T_{liq} indicate the solidus and liquidus temperatures respectively. Due to the onset of magnetic ordering in this alloy, the data points represent the electrical resistivity only above ca. 1370 K.

Here the sample radius *a* was set to its known value at room temperature. As a precaution, the heating phase data have been excluded from the evaluation, because the higher magnetic pressure $p_{mag} \propto I_0^2$ during heating, see Fig. 3, may deform the supposed sphericity of the sample too much. Above ca. 1350 K in the solid and ca. 1370 K in the liquid state the mean values of the resistivity data of $Co_{80}Pd_{20}$ fit perfectly to the linear temperature dependencies given by:

$$r_{sol}(T) = 122 + 0.042 \cdot (T - 1563) \quad [m\Omega cm]$$

$$r_{liq}(T) = 146 + 0.050 \cdot (T - 1613) \quad [m\Omega cm].$$

(12)

Below these temperatures the data points deviate at first weakly and then strongly from this behavior, indicating the onset of a magnetic ordering. In this temperature range the data points may no longer be interpreted as resistivities, because the applied inductive measurement technique reacts also very sensitive to ferromagnetic sample properties, which are, however, not considered in the above formulas.

5. SUMMARY

Electromagnetic levitation in combination with low gravity yields a good basis for simple and precise measurements of thermophysical quantities of metallic melts. Indeed, this combination enabled for the first time the measurement of viscosity and electrical resistivity of a metallic melt, here $Co_{80}Pd_{20}$, in the undercooled state. The main reason is, that the measuring process is not disturbed by external volume forces acting on the liquid sample. The almost continuous recording (10 Hz) of the electrical measurement quantities, U_0 and I_0, allowed also a detailed observation of the magnetic behavior of the liquid undercooled $Co_{80}Pd_{20}$ alloy. Unfortunately we could not record viscosity or surface tension data points within the small magnetic temperature range of

the melt. Thus, we could not verify whether the magnetic ordering is also accompanied with structural changes in the liquid.

ACKNOWLEDGMENTS

REFERENCES

1. D. Platzek, C. Notthoff, D.M. Herlach, G. Jacobs, D. Herlach, and K. Maier, *Appl. Phys. Lett.* **65:** 1723 (1994).

2. J. Reske, D.M. Herlach, F. Keuser, K. Maier, and D. Platzek, *Phys Rev. Lett.* **75:** 737 (1995).

3. M.J.P. Nijmeijer and J.J. Weis, *Phys Rev. Lett.* **75:** 2887 (1995).

4. B. Groh and S. Dietrich, *Phys Rev. Lett.* **79:** 749 (1997).

5. I. Egry, G. Lohöfer, and S. Sauerland, *Int. J. Thermophys.* **14:** 573 (1993).

6. E.C. Okress, D.M. Wroughton, G. Comenetz, P.H. Brace, and J.C.R. Kelly, *J. Appl. Phys.* **23:** 545 (1952).

7. G. Lohöfer, *SIAM J. Appl. Math.* **49:** 567 (1989).

8. Lord Rayleigh, *Proc. Roy. Soc.* **29:**: 71 (1879).

9. D.L. Cummings and D.A. Blackburn, *J. Fluid Mech.* **224:** 395 (1991).

10. S. Chandrasekhar, Hydrodynamic and Hydromagnetic Stability (Dover, New York, 1961).

11. A. Bratz and I. Egry, *J. Fluid Mech.* **298:** 341 (1995).

12. G. Lohöfer, *Int. J. Engng Sci.*, **32:** 107 (1994).

13. G. Lohöfer and I. Egry, in Solidification 1999 (The Minerals, Metals & Materials Society, Warrendale, 1999, p. 65).

14. T. Richardsen and G. Lohöfer, *Int. J. Thermophys.* **20:** 1029 (1999).